

PRIMARY AND SECONDARY PHENOMENA DURING RF-PROCESSING OF ELECTRON LINAC STRUCTURES

A.N.Dovbnya, V.F.Zhiglo, Kharkov Institute of Physics & Technology 310108 Kharkov Ukraine

1. INTRODUCTION

Breakdowns are inevitable at the switching on of accelerators or after changing their operation mode. Multiple breakdowns are brought about purposefully during an rf-processing. With this in mind, the notion of a limiting field make sense only in the case of a stable vacuum insulation state which sets-in after multiple breakdowns. The termination of an rf-processing would, logically, be the moment at which the mentioned state is determined by breakdown produced emitters, i.e. the secondary ones. Detection of such a state in vacuum insulation and its investigation, is valuable for development of limiting field enhancement methods and estimation of accessible fields in real conditions. In this work we try to discover certain phenomena associated with secondary breakdowns in dc- and rf-fields.

2. METHODS AND EQUIPMENT

Breakdown phenomena in accelerators were studied by acoustical breakdown location [2] with an accuracy ± 0.15 m and resolution of simultaneous breakdowns 2 m. Studies on vacuum insulation under various techniques of surface finish require a great number of measurements to be taken at identical vacuum conditions. Considering this, such studies were done at dc-voltage. The vacuum gap between plane-parallel electrodes being 0.05 cm, the shunting capacitance 3 nF and the power supply resistance 10 MOm. The vacuum chamber containing 22 pairs of electrodes had been baked up to 250°C for 18 hours at a pressure 10^{-3} Pa prior to voltage application. RF-breakdowns were studies on S-bang traveling wave structures. Nitrogen trap and Pennings pumps were used in vacuum systems. The preliminary machining was done using diamond cutters with the following acetone and alcohol washing. The surface polishing by Ar^+ -ions was performed by beam incident on to the rotating target at grazing angle [3]. TiN surface coating 2-10 μ m thick were deposits using the plasma-aided ion deposition method providing for strong adhesion. Experimental techniques were picked such as to be promising in the accelerator technology.

3. RESULTS AND DISCUSSIONS

3.1. Breakdown Frequency as a Field Strength Function

In most cases similarly for [4], two characteristic peaks 1 and 2 were observed (Fig.1) following which there was a decrease in the breakdown field.

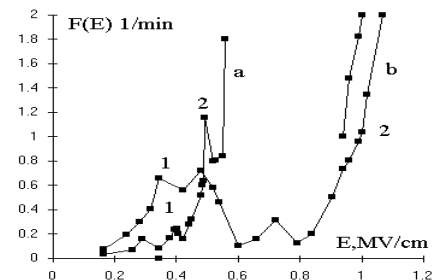


Fig.1. Breakdown frequency versus electric field
a - rf-, b - dc-field

In the rf-case, the peak 2 region was characterized by appearance of serial breakdowns whose repetition rate coincided with that of rf-pulses. That was often accompanied by a decrease in the breakdown field so that further rf-processing could be done only after the shortening of rf-pulses from 2.5 μ s to 1.0-0.5 μ s. DC-dark current measurements indicated that the breakdown accompanied by a current jump. Notably characteristic of the region 1 was jumps decreasing a current, while the region 2 its increasing, as rule. Behind the peak 2 occurred a gradual current buildup overloaded the power supply unit. The F-N straight lines, measured in the region 1 upon voltage ups and downs did not coincide as demonstrated in Fig.2.

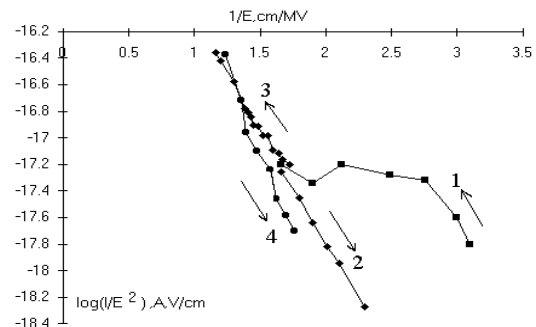


Fig.2. F-N plots in the field 1 region

1,2 - before, 3,4 - after the first breakdown

The measurement time was approximately 5-10 s, being insufficient for re-shaping of the emitter geometry. The F-N straight lines slope during voltage rise was always smaller than its decrease. In the region 2, the F-N straight lines were, as rule, reproduced during voltage down- and up climb. The processing was terminated by emergence of high-emission states like [6] which overloaded the power supply unit and spoiled the vacuum. Such states remained for 10-30 days at pressure 1 Pa after turning-off the device. Repeated turning-on of the device indicated the recovery of the initial processing states. However, several breakdowns (at time even one) were enough to cause a recurrence of high-emission state. It is this moment that we considered to be the end of the processing. The change of nature of the vacuum insulation in the high field region 2 can be accounted for by appearance of the secondary emission points. The dynamics of F-N straight lines in the region 1 indicates a decrease in the electron work function during absence of the current and its increase under influence of the current. Such a result does not agree with the adsorption-desorption work function variation model [5] from which it follows that the work function increases when gases adsorb during the current lapse and decreases under the current action. As different from above, the model of field emission from thin films [1] does not contradict our data, since the presence of films leads to, reduction of electron work function in proportion to their thickness. The reproducibility of F-N plots in the region 2 indicates that secondary emitters are stable under the action of current. This phenomenon can be associated with the complete surface purification as a result of emitter meltdown or with appearance of carbides or other refractory carbon composites [6]. The first assumption is not confirmed by the duration of the emitter initial state recovery (10-20 days) that does not match the duration of adsorption (10-20 minutes) [5].

The emitting surface can be described by the emitter distribution function along the enhancement factor $f(\beta)$. Here $\beta = \beta_1 \beta_2$ and β_1, β_2 are determined by the shape and purity of the emitter [1], respectively. At the field E the breakdowns are initiated by emitters which has $\beta(E) = E_{cr} / E$, where E_{cr} is critical field ($\approx 6 \times 10^9$ V/m). The number of breakdowns during field variation from 0 to E :

$$n(E) = -n_0 \int_0^E f(\beta) \frac{\partial \beta}{\partial E} dE,$$

and their frequency $F(E) = dn/dt$, or:

$$F(E) = n_0 f(\beta) \beta^2 (1/E_{cr}) \partial E / \partial t \quad (1)$$

The function $f(\beta)$ can be represented as

$$f(\beta) = f_1(\beta_p) + f_2(\beta_s) \text{ with peaks at } \beta_p^m \text{ and } \beta_s^m.$$

Peaks 1 and 2 for $F(E)$ follow from (1). Breakdown field decrement can be at $\beta_s^m > \beta_p^m$ or at least, during the

crossover of f_1 - and f_2 - distributions. In last case, the initiation of both primary and secondary breakdowns is possible.

3.2. Breakdown Frequency and Technology

To our mind, only two secondary emitter types can exist on the contaminated surface: $\beta_s = \beta_{1p} \beta_{2s}$ and $\beta_s = \beta_{1s} \beta_{2s}$. The first one is associated with impurity activation on the original surface. The second one represents secondary emitter appearance upon the site of a primary emitter explosion. If the original surface roughness is characterized by the average protrusion height R_z , then $\beta_{1p} \sim R_z^\alpha, \alpha > 0$. The surface sorption is known to increase with R_z , and therefore $\beta_{2p} \sim R_z^\gamma, \beta_{2s} \sim R_z^\delta, \gamma, \delta > 0$. Experiments indicate β_{1s} is little technology-dependent, being determined, in main, by parameters of the power feed circuit [4], i.e. $\beta_{1s} = \text{const}$. Hence $\beta_p = \beta_{1p} \beta_{2p} \sim R_z^{\alpha+\gamma}, \beta_s \sim R_z^{\alpha+\delta}$ or $\beta_s \sim R_z^\gamma$.

For a clean surface: $\beta_{2p} = 1, \beta_{2s} = 1, \beta_s = \beta_{1s} \beta_{2s} = \text{const}$, and $\beta_p \sim R_z^\alpha$. The position of breakdown frequency peaks corresponding to the dynamics β_p and β_s is shown in Fig.3, Fig.4 in case $\partial \beta_s / \partial R_z > \partial \beta_p / \partial R_z$.

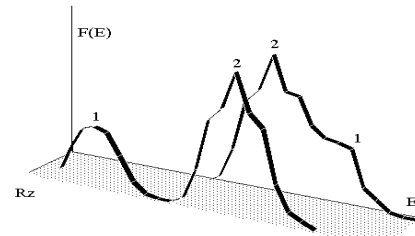


Fig.3. Breakdown frequency at a clean surface

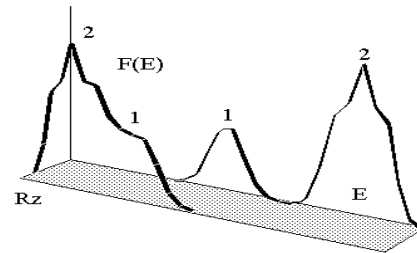


Fig.4. Breakdown frequency at a contaminated surface

From comparison of the experimental results in Fig.5 with data in Fig.3 and Fig.4 one can deduce that the breakdown field is limited for the technologies under investigation by surface impurities. This agrees well with the conclusion made from the dark current measurements in Article 3.1. The results for TiN indicate an essential role of electrodes material in

initiating not only the primary, but also the secondary breakdowns.

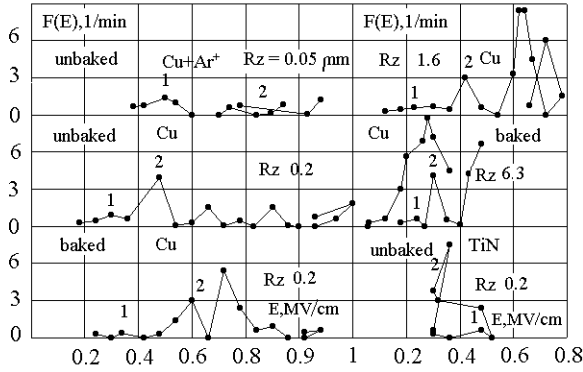


Fig.5. Breakdown frequency at various technologies

3.3. Breakdown Distribution in the Linac

In the beginning of the rf-processing, the breakdown distribution was homogeneous under fields ~ 100 - 200 kV/cm. Upon further field increase there appeared a peak of the breakdown in the input coupler, i.e. in the high field region. In the section with a constant field decay factor, such a peak moved gradually towards the load as the field grew higher, i.e. to the low field region. This fact can be taken for the surface impurity dynamics. Yet, it can be shown, the breakdown peak shift can also be associated with getting by the primary breakdown peak 1. From (1) it follows $F = F(x, t)$, if $E = E(x, t)$, i.e. there appears a spatial-temporal relationship in the breakdown distribution, event at a homogeneous impurity or in clean sections. This phenomena can be illustrated by the Gaussian distribution $F(\beta)$ and accelerating field $E = ct \exp(-\alpha x)$. In this case, the breakdown frequency is:

$$\Phi(x, E_0) = \frac{n_0 \beta \exp\left(-\frac{1}{2} \left(\frac{\beta - \beta_0}{\sigma}\right)^2\right)}{\sigma E_0 \exp(-\alpha x) \sqrt{2\pi}} \quad (2)$$

where $E_0 = ct$. This function is given in Fig.6 at the $\sigma = 66.6$, $\beta_0 = 200$, $n_0 = 2 \times 10^4 m^{-1}$, $c = 2 \times 10^4 Vm^{-1}s^{-1}$, $E_{cr} = 6.9 \times 10^9 Vm^{-1}$, $\alpha = 0.21 m^{-1}$. Clearly observable is the breakdown peak shift as the field increases.

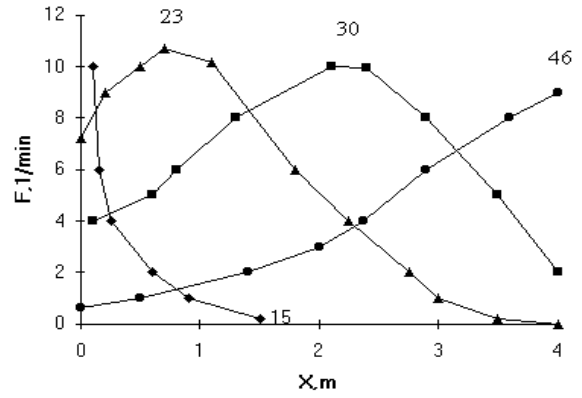


Fig.6. Breakdown longitudinal distribution in the accelerating sections at various field E_0 , MV/m

A possible secondary breakdown initiation, as caused by gas desorption and by reflecting wave can also be investigated on the longitudinal breakdown distribution. These phenomena must be manifested in the appearance of a breakdown peak in the section mid portion and simultaneous (paired) breakdowns in different parts of the accelerating section. Such phenomena were not registered. Reflecting waves presence during several rf-pulses after the breakdown [2] indicate the efficient desorbed gas ionization. Such an effect must be proportional to the pulse repetition rate and led to rf-window breakdowns. In our experiments we observed a connection between rf-window and section breakdowns. The section breakdowns always preceded rf-window breakdowns. Serial breakdowns ($F=50$ Hz) always ended in window breakdowns.

4. REFERENCES

1. G.A.Loew, J.W.Wang. Field emission and rf-breakdown in the copper accelerator structures. SLAC-PUB-5059. August 1989.
2. E.Z.Biller et al. Electrical reliability and the rf-breakdowns in accelerator sections. 13-th Int. Symp. on DEIV, Paris 1988, p.500.
3. V.F.Zhiglo, B.A.Terechov. Polishing of copper with Ar^+ ions. VANT Ser. Techn. of Phys. exper, v.2(60), p.40, Kharkov 1980 (in Russia)
4. I.N.Slivkov. High voltage processes in vacuum. Energoatomizdat, Moskow 1986 (in Russia).
5. H.Powell, P.Chatterton. Prebreakdown conduction between vacuum insulated electrodes. Vacuum v.20, N10, p.419, 1970.
6. F.G.Zheleznikov et al. About a nature of the electron load in accelerating tubes of electrostatic accelerators. Zhur. Technicheskoy Physiki v.43, p.2194, 1973.